

Article

Results from the Cuore Experiment [†]

Alessio Caminata ^{1,*} , Douglas Adams ², Chris Alduino ², Krystal Alfonso ³, Frank Avignone III ², Oscar Azzolini ⁴, Giacomo Bari ⁵, Fabio Bellini ^{6,7} , Giovanni Benato ⁸, Andrea Bersani ¹, Matteo Biassoni ⁹, Antonio Branca ^{10,11}, Chiara Brofferio ^{9,12}, Carlo Bucci ¹³, Alice Campani ^{1,14}, Lucia Canonica ^{13,15}, Xi-Guang Cao ¹⁶, Silvia Capelli ^{9,12}, Luigi Cappelli ^{8,13,17}, Laura Cardani ⁷, Paolo Carniti ^{9,12}, Nicola Casali ⁷, Davide Chiesa ^{9,12}, Nicholas Chott ², Massimiliano Clemenza ^{9,12}, Simone Copello ^{13,18}, Carlo Cosmelli ^{6,7}, Oliviero Cremonesi ⁹, Richard Creswick ², Jeremy Cushman ¹⁹, Antonio D'Addabbo ¹³, Damiano D'Aguanno ^{13,20}, Ioan Dafinei ⁷, Christopher Davis ¹⁹, Stefano Dell'Oro ²¹, Milena Deninno ⁵, Sergio Di Domizio ^{1,14}, Valentina Dompè ^{13,18}, Alexey Drobizhev ^{8,17}, De-Qing Fang ¹⁶, Guido Fantini ^{13,18}, Marco Faverzani ^{9,12}, Elena Ferri ^{9,12}, Fernando Ferroni ^{6,7}, Ettore Fiorini ^{9,12}, Massimo Alberto Franceschi ²², Stuart Freedman ^{8,17,†}, Brian Fujikawa ¹⁷, Andrea Giachero ^{9,12} , Luca Gironi ^{9,12} , Andrea Giuliani ²³, Paolo Gorla ¹³, Claudio Gotti ^{9,12} , Thomas Gutierrez ²⁴, Ke Han ²⁵, Karsten Heeger ¹⁹, Raul Hennings-Yeomans ^{8,17}, Roger Huang ⁸, Huan Zhong Huang ³, Joe Johnston ¹⁵, Giorgio Keppel ⁴ , Yury Kolomensky ^{8,17}, Alexander Leder ¹⁵, Carlo Ligi ²², Yu-Gang Ma ¹⁶, Laura Marini ^{8,17}, Maria Martinez ^{6,7,26}, Reina Maruyama ¹⁹, Yuan Mei ¹⁷, Niccolò Moggi ^{5,27}, Silvio Morganti ⁷, Tommaso Napolitano ²², Massimiliano Nastasi ^{9,12}, Claudia Nones ²⁸, Eric Norman ^{29,30}, Valentina Novati ²³, Angelo Nucciotti ^{9,12}, Irene Nutini ^{13,18}, Thomas O'Donnell ²¹, Jonathan Ouellet ¹⁵, Carmine Pagliarone ^{13,20}, Marco Pallavicini ^{1,14}, Luca Pattavina ¹³, Maura Pavan ^{9,12}, Gianluigi Pessina ⁹, Valerio Pettinacci ⁷, Cristian Pira ⁴, Stefano Pirro ¹³, Stefano Pozzi ^{9,12}, Ezio Previtali ⁹ , Andrei Puiu ^{9,12}, Carl Rosenfeld ², Claudia Rusconi ^{2,13} , Michinari Sakai ³, Samuele Sangiorgio ²⁹, Benjamin Schmidt ¹⁷, Nick Scielzo ²⁹, Vivek Singh ⁸, Monica Sisti ^{9,12}, Danielle Speller ¹⁹, Luca Taffarello ¹⁰, Francesco Terranova ^{9,12}, Claudia Tomei ⁷, Marco Vignati ⁷, Sachintha Wagaarachchi ^{8,17}, Barbara Wang ^{29,30}, Bradford Welliver ¹⁷, Jeffrey Wilson ², Kevin Wilson ², Lindley Winslow ¹⁵, Tom Wise ^{19,32}, Luigi Zanotti ^{9,12} , Sergio Zimmermann ³³, and Stefano Zucchelli ^{5,27}

¹ Istituto Nazionale di Fisica Nucleare (INFN)—Sezione di Genova, I-16146 Genova, Italy; andrea.bersani@ge.infn.it (A.B.); alice.campani@ge.infn.it (A.C.); sergio.didomizio@ge.infn.it (S.D.D.); marco.pallavicini@ge.infn.it (M.P.)

² Department of Physics and Astronomy, University of South Carolina, Columbia, SC 29208, USA; da2@email.sc.edu (D.A.); alduino@email.sc.edu (C.A.); titus3@mac.com (F.A.III); chott@email.sc.edu (N.C.); creswick.rj@sc.edu (R.C.); lcr@sc.edu (C.R.); claudia.rusconi@mib.infn.it (C.R.); jrwilso2@mailbox.sc.edu (J.W.); kwilson@sc.edu (K.W.)

³ Department of Physics and Astronomy, University of California, Los Angeles, CA 90095, USA; kalfonso@ucla.edu (K.A.); huang@physics.ucla.edu (H.Z.H.); michsakai@ucla.edu (M.S.);

⁴ Istituto Nazionale di Fisica Nucleare (INFN)—Laboratori Nazionali di Legnaro, I-35020 Legnaro (Padova), Italy; oscar.azzolini@lnl.infn.it (O.A.); giorgio.keppel@lnl.infn.it (G.K.); cristian.pira@lnl.infn.it (C.P.)

⁵ Istituto Nazionale di Fisica Nucleare (INFN)—Sezione di Bologna, I-40127 Bologna, Italy; giacomo.bari@lngs.infn.it (G.B.); deninno@bo.infn.it (M.D.); niccolo.moggi@bo.infn.it (N.M.); stefano.zucchelli@bo.infn.it (S.Z.)

⁶ Dipartimento di Fisica, Sapienza Università di Roma, I-00185 Roma, Italy; Fabio.Bellini@roma1.infn.it (F.B.); carlo.cosmelli@roma1.infn.it (C.C.); fernando.ferroni@roma1.infn.it (F.F.); mariam@unizar.es (M.M.)

⁷ Istituto Nazionale di Fisica Nucleare (INFN)—Sezione di Roma, I-00185 Roma, Italy; laura.cardani@roma1.infn.it (L.C.); nicola.casali@roma1.infn.it (N.C.); ioan.dafinei@roma1.infn.it (I.D.); silvio.morganti@roma1.infn.it (S.M.); valerio.pettinacci@roma1.infn.it (V.P.); claudia.tomei@roma1.infn.it (C.T.); marco.vignati@roma1.infn.it (M.V.)

- ⁸ Department of Physics, University of California, Berkeley, CA 94720, USA; gbenato@berkeley.edu (G.B.); luigi.cappelli@lngs.infn.it (L.C.); adrobizhev@lbl.gov (A.D.); SJFreedman@lbl.gov (S.F.); hennings@berkeley.edu (R.H.-Y.); roger_huang@berkeley.edu (R.H.); ygkolomensky@lbl.gov (Y.K.); lmarini@berkeley.edu (L.M.); singhv@berkeley.edu (V.S.); sachi@berkeley.edu (S.W.)
- ⁹ Istituto Nazionale di Fisica Nucleare (INFN)—Sezione di Milano Bicocca, I-20126 Milano, Italy; matteo.biassoni@mib.infn.it (M.B.); chiara.brofferio@mib.infn.it (C.B.); silvia.capelli@mib.infn.it (S.C.); paolo.carniti@mib.infn.it (P.C.); davide.chiesa@mib.infn.it (D.C.); massimiliano.clemenza@mib.infn.it (M.C.); oliviero.cremonesi@mib.infn.it (O.C.); marco.faverzani@mib.infn.it (M.F.); elena.ferri@mib.infn.it (E.F.); ettore.fiorini@mib.infn.it (E.F.); andrea.giachero@mib.infn.it (A.G.); luca.gironi@mib.infn.it (L.G.); claudio.gotti@mib.infn.it (C.G.); massimiliano.nastasi@mib.infn.it (M.N.); angelo.nucciotti@mib.infn.it (A.N.); maura.pavan@mib.infn.it (M.P.); gianluigi.pessina@mib.infn.it (G.P.); stefano.pozzi@mib.infn.it (S.P.); ezio.previtalli@mib.infn.it (E.P.); andrei.puiu@mib.infn.it (A.P.); monica.sisti@mib.infn.it (M.S.); francesco.terranova@mib.infn.it (F.T.); luigi.zanotti@mib.infn.it (L.Z.)
- ¹⁰ Istituto Nazionale di Fisica Nucleare (INFN)—Sezione di Padova, I-35131 Padova, Italy; branca@pd.infn.it (A.B.); luca.taffarello@pd.infn.it (L.T.)
- ¹¹ Dipartimento di Fisica e Astronomia, Università di Padova, I-35131 Padova, Italy
- ¹² Dipartimento di Fisica, Università di Milano—Bicocca, I-20126 Milano, Italy
- ¹³ Istituto Nazionale di Fisica Nucleare (INFN)—Laboratori Nazionali del Gran Sasso, I-67100 Assergi (L’Aquila), Italy; carlo.bucci@lngs.infn.it (C.B.); lucia.canonica@lngs.infn.it (L.C.); simone.copello@ge.infn.it (S.C.); antonio.daddabbo@lngs.infn.it (A.D.); damiano.daguanno@unicas.it (D.D.); valentina.dompe@gssi.it (V.D.); guido.fantini@gssi.it (G.F.); paolo.gorla@lngs.infn.it (P.G.); irene.nutini@gssi.infn.it (I.N.); carmine.pagliarone@lngs.infn.it (C.P.); luca.pattavina@lngs.infn.it (L.P.); stefano.pirro@lngs.infn.it (S.P.)
- ¹⁴ Dipartimento di Fisica, Università di Genova, I-16146 Genova, Italy
- ¹⁵ Laboratory for Nuclear Science, Massachusetts Institute of Technology, Cambridge, MA 02139, USA; jpp13@mit.edu (J.J.); aleder@mit.edu (A.L.); ouelletj@mit.edu (J.O.); lwinslow@mit.edu (L.W.)
- ¹⁶ Shanghai Institute of Applied Physics, Chinese Academy of Sciences, Shanghai 201800, China; caoxiguang@sinap.ac.cn (X.-G.C.); fangdeqing@sinap.ac.cn (D.-Q.F.); ygma@sinap.ac.cn (Y.-G.M.)
- ¹⁷ Nuclear Science Division, Lawrence Berkeley National Laboratory, Berkeley, CA 94720, USA; bkfujikawa@lbl.gov (B.F.); ymei@lbl.gov (Y.M.); beschmidt@lbl.gov (B.S.); bcwelliver@lbl.gov (B.W.)
- ¹⁸ Istituto Nazionale di Fisica Nucleare (INFN)—Gran Sasso Science Institute, I-67100 L’Aquila, Italy
- ¹⁹ Wright Laboratory, Department of Physics, Yale University, New Haven, CT 06520, USA; jeremy.cushman@yale.edu (J.C.); christopher.davis@yale.edu (C.D.); karsten.heeger@yale.edu (K.H.); reina.maruyama@yale.edu (R.M.); danielle.speller@yale.edu (D.S.); wise@physics.wisc.edu (T.W.)
- ²⁰ Dipartimento di Ingegneria Civile e Meccanica, Università degli Studi di Cassino e del Lazio Meridionale, I-03043 Cassino, Italy
- ²¹ Center for Neutrino Physics, Virginia Polytechnic Institute and State University, Blacksburg, VA 24061, USA; sdelloro@vt.edu (S.D.); tdonnell@vt.edu (T.O.)
- ²² Istituto Nazionale di Fisica Nucleare (INFN)—Laboratori Nazionali di Frascati, I-00044 Frascati (Roma), Italy; alberto.franceschi@lnf.infn.it (M.A.F.); carlo.ligi@lnf.infn.it (C.L.); tommaso.napolitano@lnf.infn.it (T.N.)
- ²³ CSNSM, University of Paris-Sud, CNRS/IN2P3, Université Paris-Saclay, 91405 Orsay, France; andrea.giuliani@csnsm.in2p3.fr (A.G.); valentina.novati@csnsm.in2p3.fr (V.N.)
- ²⁴ Physics Department, California Polytechnic State University, San Luis Obispo, CA 93407, USA; tdgutier@calpoly.edu
- ²⁵ INPAC and School of Physics and Astronomy, Shanghai Jiao Tong University, Shanghai Laboratory for Particle Physics and Cosmology, Shanghai 200240, China; ke.han@sjtu.edu.cn
- ²⁶ Laboratorio de Física Nuclear y Astroparticulas, Universidad de Zaragoza, 50009 Zaragoza, Spain
- ²⁷ Dipartimento di Fisica e Astronomia, Alma Mater Studiorum—Università di Bologna, I-40127 Bologna, Italy;
- ²⁸ Service de Physique des Particules, CEA/Saclay, 91191 Gif-sur-Yvette, France; claudia.nones@cea.fr
- ²⁹ Lawrence Livermore National Laboratory, Livermore, CA 94550, USA; EBNorman@lbl.gov (E.N.); samuele@llnl.gov (S.S.); scielzo1@llnl.gov (N.S.); alan2@llnl.gov (B.W.)
- ³⁰ Department of Nuclear Engineering, University of California, Berkeley, CA 94720, USA
- ³¹ Dipartimento di Scienze Fisiche e Chimiche, Università dell’Aquila, I-67100 L’Aquila, Italy
- ³² Department of Physics, University of Wisconsin, Madison, WI 53706, USA

³³ Engineering Division, Lawrence Berkeley National Laboratory, Berkeley, CA 94720, USA; SZimmermann@lbl.gov

* Correspondence: alessio.caminata@ge.infn.it

† This paper is based on the talk at the 7th International Conference on New Frontiers in Physics (ICNFP 2018), Crete, Greece, 4–12 July 2018.

‡ Deceased.

Received: 30 November 2018; Accepted: 26 December 2018; Published: 2 January 2019

Abstract: The Cryogenic Underground Observatory for Rare Events (CUORE) is the first bolometric experiment searching for neutrinoless double beta decay that has been able to reach the 1-ton scale. The detector consists of an array of 988 TeO₂ crystals arranged in a cylindrical compact structure of 19 towers, each of them made of 52 crystals. The construction of the experiment was completed in August 2016 and the data taking started in spring 2017 after a period of commissioning and tests. In this work we present the neutrinoless double beta decay results of CUORE from examining a total TeO₂ exposure of 86.3 kg yr, characterized by an effective energy resolution of 7.7 keV FWHM and a background in the region of interest of 0.014 counts/(keV kg yr). In this physics run, CUORE placed a lower limit on the decay half-life of neutrinoless double beta decay of ¹³⁰Te > 1.3 · 10²⁵ yr (90% C.L.). Moreover, an analysis of the background of the experiment is presented as well as the measurement of the ¹³⁰Te 2νββ decay with a resulting half-life of $T_{1/2}^{2\nu} = [7.9 \pm 0.1 \text{ (stat.)} \pm 0.2 \text{ (syst.)}] \times 10^{20} \text{ yr}$ which is the most precise measurement of the half-life and compatible with previous results.

Keywords: neutrinoless double beta decay; CUORE; Majorana Neutrino

1. Introduction

Double beta decay is a rare process in which a nucleus (A, Z) decays to $(A, Z + 2) + 2e^- + 2\bar{\nu}$. This process is allowed by the Standard Particle models, although it is very rare. After the discovery of neutrino flavor oscillations in the early 2000s [1–5] and the consecutive deduction that neutrinos are not massless particles, the search for rare nuclear decays to infer the neutrino mass had a considerable boost [6]. In spite of about 20 years of searches so far, neither the scale nor the nature of the neutrino mass are clear. In fact, the neutrino could have either a Dirac or a Majorana mass type. In the latter case, it would imply violation of the lepton quantum number and new physics beyond the Standard Model. Moreover, it would have an implication for the matter-antimatter asymmetry of the Universe. It is worth noting that, if neutrinos are Majorana particles, neutrinoless double beta decay ($0\nu\beta\beta$) can take place. It is a so far unobserved nuclear process in which a nucleus (A, Z) decays to $(A, Z + 2) + 2e^-$, manifestly violating lepton number conservation.

The Cryogenic Underground Observatory for Rare Events (CUORE) experiment has the search of the neutrinoless double beta decay of ¹³⁰Te to ¹³⁰Xe + 2e⁻ as its main scientific goal [7]. In the case of a positive signal, this would be a conclusive indication that the neutrinos are Majorana particles. Moreover, it would provide a measurement of the neutrino mass. The search for neutrinoless double beta decay is a very active field of research with several collaborations around the world looking for it with several techniques (e.g., Ge-diodes [8], liquid scintillators [9,10], and TPCs [11]). CUORE is the first tonne-scale experiment for the search of neutrinoless double beta decay with cryogenic techniques. It was designed based on the experience of previous demonstrators and experiments [12–16] and it is currently in the data taking phase at Laboratori Nazionali del Gran Sasso (central Italy).

In neutrinoless double beta decay searches, the figure of merit that drives the sensitivity can be expressed as $\sim \epsilon \sqrt{MT/(b\Delta E)}$ where ϵ is the total signal efficiency, M is the active mass, T is the live time, b is in background in counts/(keV · kg · yr) around the endpoint of the double beta decay spectrum ($Q_{\beta\beta}$) and ΔE is the energy resolution [17]. CUORE aims for an energy resolution of about $\Delta E \sim 5$ keV full-width half-maximum (FWHM) at $Q_{\beta\beta}$ and a background index b of about

0.01 counts/(keV · kg · yr) [18]. The ultimate CUORE sensitivity to the half life of ^{130}Te neutrinoless double beta decay after five years of livetime is 9×10^{25} yr.

2. Detector Design and Construction

The CUORE detector consists of 988 bolometers operating independently, with each bolometer acting as an individual detector searching for $0\nu\beta\beta$ decay. In this experimental configuration, the crystal acts as both the source and detector of the decays of interest. A CUORE bolometer is composed of two main components: an absorber (the crystal), which absorbs the energy released in a particle interaction increasing consequently its temperature, and a thermistor, which converts this change in temperature into a measurable change in voltage (see Figure 1). A CUORE absorber is a Tellurium oxide crystal, $5 \times 5 \times 5 \text{ cm}^3$ in size and about 750 g in mass. Thanks to the relatively high ^{130}Te isotopic abundance, the crystal is made using $^{\text{nat}}\text{Te}$. Crystals absorb the kinetic energy of the electrons emitted by the decay while neutrinos free stream out of the detectors. Consequently, searching for $0\nu\beta\beta$ implies looking for a peak at the endpoint of the ^{130}Te decay, $Q_{\beta\beta} = 2527.5 \text{ keV}$. This source = detector configuration gives us a high signal efficiency of around 85% (full containment of both the emitted electrons in a single crystal).

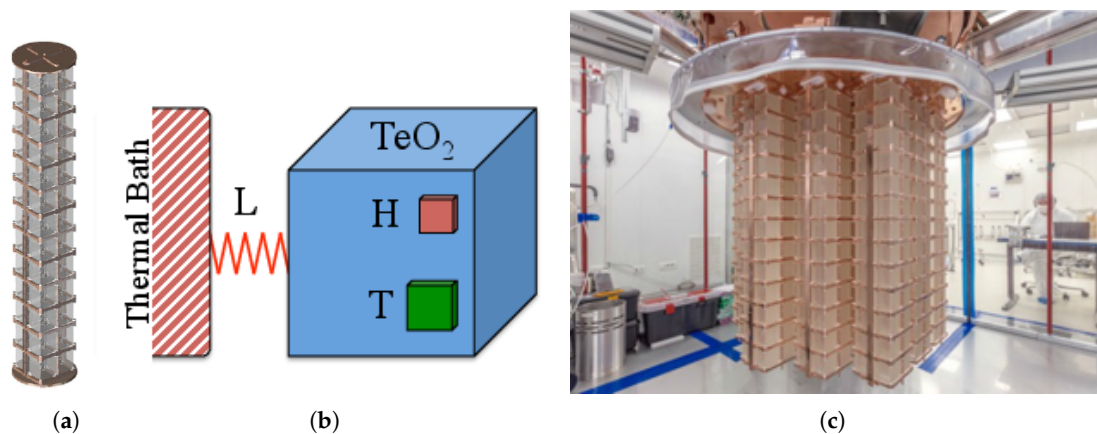


Figure 1. (a) Schematic of a single Cryogenic Underground Observatory for Rare Events (CUORE) tower, with 13 floors of four crystals. Each tower has 52 crystals for a total mass of $\sim 39 \text{ kg}$ of TeO_2 or $\sim 10.8 \text{ kg}$ of ^{130}Te . The CUORE detector is composed of 19 such towers. (b) A schematic of a CUORE bolometer. The TeO_2 crystal acts as the absorber, and is connected to a heat bath through a weak thermal link, L . Each bolometer is instrumented with an NTD thermistor, N , and a heater to inject heat pulses, H . (c) The CUORE detector assembled and installed in the CUORE cryostat, inside the CUORE cleanroom. Picture from [19].

In the CUORE detector, crystals are arranged into a cylindrical array of 19 towers, each containing 52 crystals over 13 floors (four crystals per floor). Each crystal has a mass of $\sim 750 \text{ g}$, for a total TeO_2 mass of 741 kg ($\sim 206 \text{ kg}$ is ^{130}Te). In order to profit from the $C \propto T^3$ of dielectric materials (Debye Law, C heat capacity, T temperature), the detector is contained in a powerful dilution-unit cryostat [20] at a temperature of about 10 mK (Figure 1). Thanks to the low operating temperature, the crystal temperature increases by about $100 \mu\text{K}$ for an energy deposit of 1 MeV .

The crystal is thermally coupled to a neutron transmutation doped thermistor (NTD) with a resistivity that is exponentially dependent on temperature. Consequently, a $\sim 1\%$ temperature change causes a $\sim 10\%$ change in resistivity. The NTDs have typical resistances of $\sim (0.1\text{--}1) \text{ G}\Omega$ and are current biased and read out using room temperature electronics.

To suppress external γ -ray backgrounds, two lead shields are integrated into the cryogenic volume: a 30-cm thick shield at $\sim 50 \text{ mK}$ above the detectors and a 6-cm thick shield at $\sim 4 \text{ K}$ around and below the detectors. The lateral and lower shields are made from ancient Roman lead with

extremely low levels of radioactivity [21]. Moreover, an external lead shield (25 cm thick) surrounded by borated polyethylene and boric acid (20 cm thick) ensures additional shielding.

The construction of the CUORE towers was completed in summer 2014 and the commissioning of the cryostat was completed two years later. The detector was then installed into the cryostat inside a specially built anti-radon tent in order to minimize the exposure to radon during the installation process [22]. The first CUORE cooldown started in December 2016 and reached base temperature one month later.

3. CUORE Data Taking and Neutrinoless Double Decay Searches

After a period of tests and commissioning, CUORE collected the first two datasets in summer 2017. The total exposure was $86.3 \text{ kg} \cdot \text{yr}$ of TeO_2 ($24.0 \text{ kg} \cdot \text{yr}$ of ^{130}Te). The data, which are shown in Figure 2, are characterized by an energy resolution $\Delta E = 7.7 \pm 0.5 \text{ keV}$ FWHM and a background index at $Q_{\beta\beta}$ of $b = 0.014 \pm 0.002 \text{ counts}/(\text{keV} \cdot \text{kg} \cdot \text{yr})$. In the future, an improvement of the background index is foreseen implementing more sophisticated quality cuts and an improvement of resolution as we continue refining our understanding of the CUORE cryostat. For example, resolution improved from 8.3 keV to 7.4 keV between the first two data-taking periods.

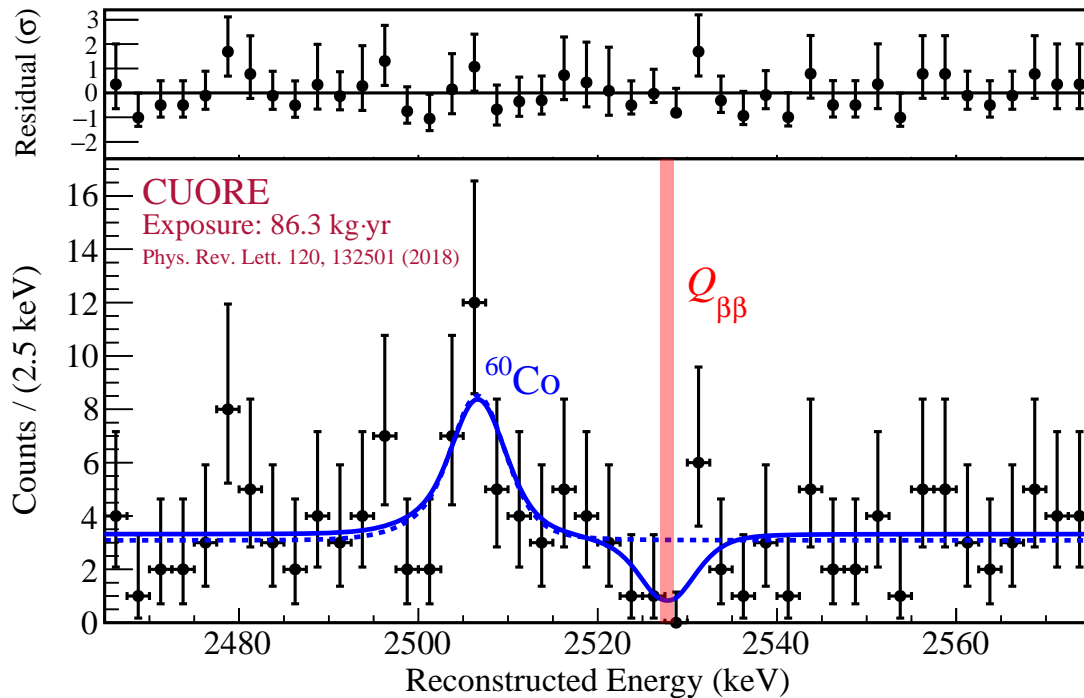


Figure 2. Left: reconstructed ^{208}Tl 2516 keV line in the calibration spectrum with residuals with data points (black) and the reconstructed line-shape (red). The dotted blue lines are the components of the line shape corresponding to different physical processes. Right: the best fit in the ROI. The value of the $Q_{\beta\beta}$ is marked in red. Picture taken from [7].

With the data collected in the first two datasets, CUORE was able to set a limit on the $0\nu\beta\beta$ half life of ^{130}Te of $T_{1/2}^{0\nu} > 1.3 \times 10^{25} \text{ yr}$ which outperforms the expected half life sensitivity ($7.6 \times 10^{24} \text{ yr}$) due to a downward fluctuation of about 2σ at $Q_{\beta\beta}$ (Figure 2). When combined with results of CUORE-0 and Cuoricino (CUORE predecessor experiments), the most stringent limit on $0\nu\beta\beta$ decay half life of ^{130}Te becomes $T_{1/2}^{0\nu} > 1.5 \times 10^{25} \text{ yr}$ at 90% C.L. [7].

4. Measurement of the $2\nu\beta\beta$ Half-Life

The same set of data used for the search for the neutrinoless double beta decay has also been used to analyze the CUORE spectrum at different energies. To understand the observed spectrum, we simulated many possible background sources from different locations in the detector using a custom Geant4-based Monte Carlo simulation [23] both close to and far from the crystal, and cosmogenic, using an approach similar to [7,24]. Data are divided into three parts: multiplicity 1 (M1) spectrum, multiplicity 2 (M2) spectrum and M2 sum spectrum ($\Sigma 2$). M1 comprises events that release all their energy in a single crystal, M2 is formed by events that release their energy in two crystals and $\Sigma 2$ is the sum of the energies of M2 events (Figure 3). Double beta decay events release their energy in a single crystal in about 90% of cases and consequently are primarily contained in the M1 spectrum. In contrast, events like γ -ray interactions and α -decays happening on the surface of a detector are usually multi-crystal events and consequently populate the M2 spectrum. Figure 3 shows the M1 and $\Sigma 2$ spectra. In the α region (reconstructed energy $\geq \sim 3$ MeV) the M1 spectrum shows several double peaks that are not present in $\Sigma 2$ spectrum. This double peak structure is due to surface contamination of surfaces near crystals with α -decaying nuclei. In this case, the α -particle is detected while the recoiled nucleus remains in the passive material. A wider discussion of this effect can be found in [24]. The M1 spectrum is further divided into M1L0 and M1L1 spectra that contain respectively the 252 inner core crystals which are expected to be more shielded from external background and the 736 external bolometers on the surface of the detector.

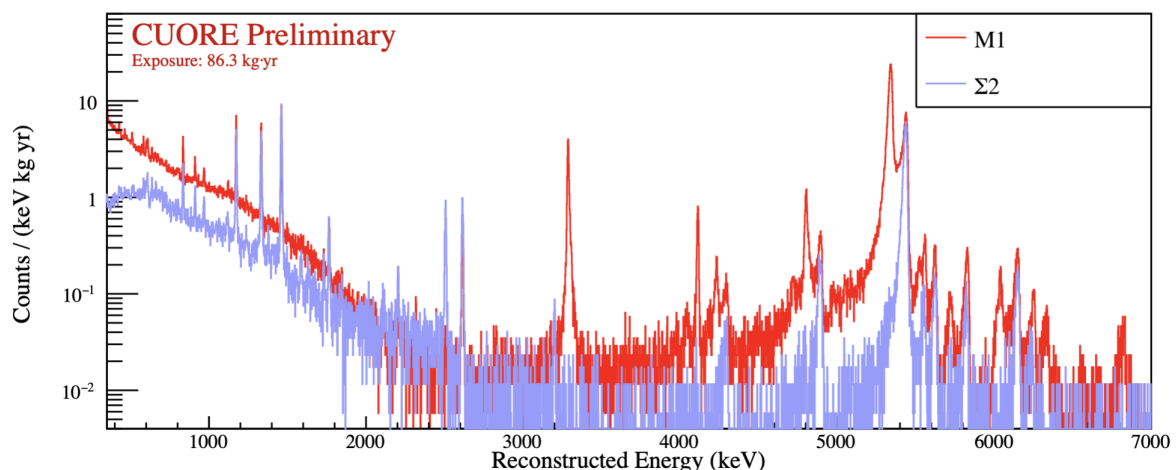


Figure 3. The CUORE M1 spectrum vs. the $\Sigma 2$ spectrum. $\Sigma 2$ is more sensitive to γ -rays interactions and surface α events. We can see this by the lack of double peaks in the α -region (reconstructed energy $\geq \sim 3$ MeV), since for an M2 event, the α and recoiling nucleus must both be detected. In case the α -particle is detected while the recoiled nucleus remains in a passive material facing the crystal, the event is detected as M1 event and forms the double peak structure. A wider discussion of this effect can be found in [24]. The peak at ≈ 3.2 MeV corresponds to the α -decay of ^{190}Pt , which is a bulk contamination of the crystal coming from its growing procedure. Since it is a bulk contamination, the full energy is typically contained in the originating crystal and the peak only appears in the M1 spectrum. Picture from [19].

We reconstruct the CUORE background by fitting the MC simulated spectra to the acquired data simultaneously across these four spectra using a Markov-Chain Monte Carlo implemented in the JAGS software package [25,26]. The fit has 60 free parameters and follows the same approach used in the CUORE-0 experiment [24]. Both the MC and observed spectra have variable bin size to reduce the effect of complicated line shapes (Figure 4).

Using data contained in the first two datasets, we were able to extract a robust measurement of the $2\nu\beta\beta$ half-life of ^{130}Te . Thanks to the improvements in the background with respect to the CUORE-0 detector (mainly coming from a better shielded cryostat) and the increased mass in analysis, $2\nu\beta\beta$ decays are the main composition of the M1 spectrum in the 1–2 MeV region (Figure 4).

To avoid biases in the tuning of the data quality cuts and fitting procedure, any comparison with previous results was avoided, blinding the MC normalization spectrum constant in order to have the extracted half-life as function of a unphysical parameter. After finalizing the cuts, we removed the blinding and we measured a half-life of ^{130}Te in the $2\nu\beta\beta$ channel of $T_{2\nu}^{1/2} = [7.9 \pm 0.1 \text{ (stat.)} \pm 0.2 \text{ (syst.)}] \times 10^{20} \text{ yr}$. The measured half-life is consistent with previous measurements [24,27].

The only component of the reconstructed model that strongly correlates with $2\nu\beta\beta$ rate is the ^{40}K decay rate in the crystal bulk (β -decays with 1310.9 keV endpoint). The same contamination was also present in CUORE-0, which has the same crystal growth procedure as CUORE crystals. However, given the large rate of $2\nu\beta\beta$ events in CUORE, this background accounts for about 1% of the signal, which is within the statistical uncertainty of the measured rate (Figure 5).

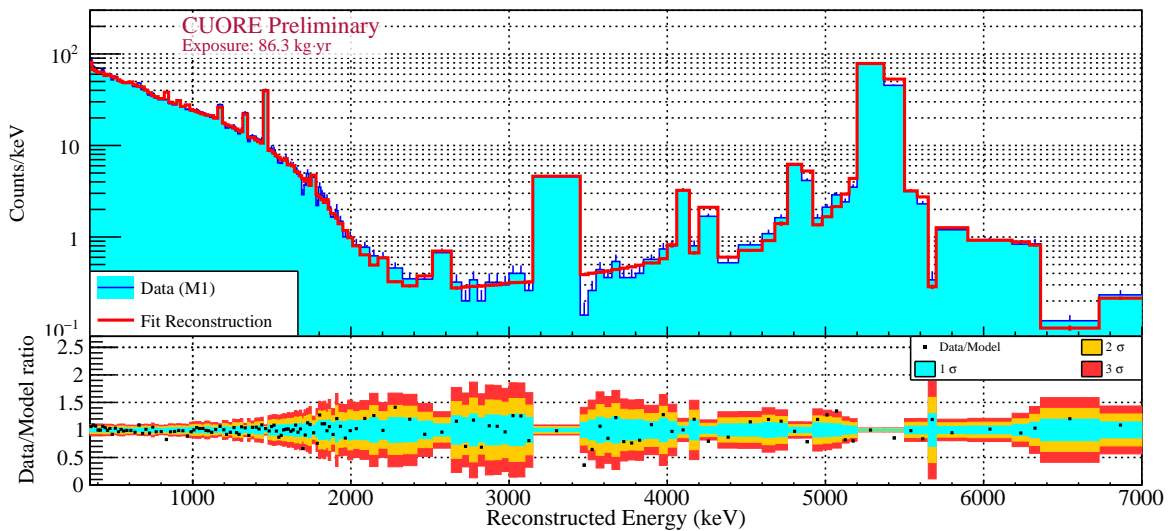


Figure 4. **Top:** M1L0 spectrum (blue) and the fit to the spectrum, built out of different simulated background components (red). The variable binning has been chosen to contain peaks into a single bin to avoid dependence on details of the peak shape while having good resolution of the model in the continuum region. **Bottom:** ratio of the data and reconstructed model with 1σ , 2σ and 3σ error bars. The continuum is well described while we have moderate disagreement in the heights of a few peaks. Picture from [19].

One of the major upgrades with respect to CUORE $0\nu\beta\beta$ analysis is the improvement of the estimation of signal acceptance efficiency. While previously we used several γ -ray lines and we were looking at the fraction of surviving events after cuts, now the M2 spectrum is considered. The previous approach was limited by the limited statistics of the events in the peaks (2.4% uncertainty contribution to the final result). Given the low event rate in CUORE, accidental M2 events are rare ($<1\%$) and constitute a clean event sample distributed over the whole energy range. Using this approach, the uncertainty on the efficiency reduces to $\approx 0.2\%$.

The systematic uncertainty ($0.2 \times 10^{20} \text{ yr}$) is dominated by the decision to split crystals between inner (contributing to M1L0) and outer (contributing to M1L1) channels. Other causes of uncertainty (energy threshold and signal efficiency) are about one order of magnitude lower. Our fit reconstruction splits the data into an inner layer of 252 bolometers and an outer layer of 736 bolometers, however, other splittings of the data are also possible and yield different results (other splittings include looking at only even or odd channels, even or odd towers, even or odd floors, the top half vs. bottom half of

the detector, etc.). The spread of the results is used to evaluate the systematic error. Different results depending on different channel grouping allow us to probe the uncertainty caused by our present ignorance of the exact location of contaminations.

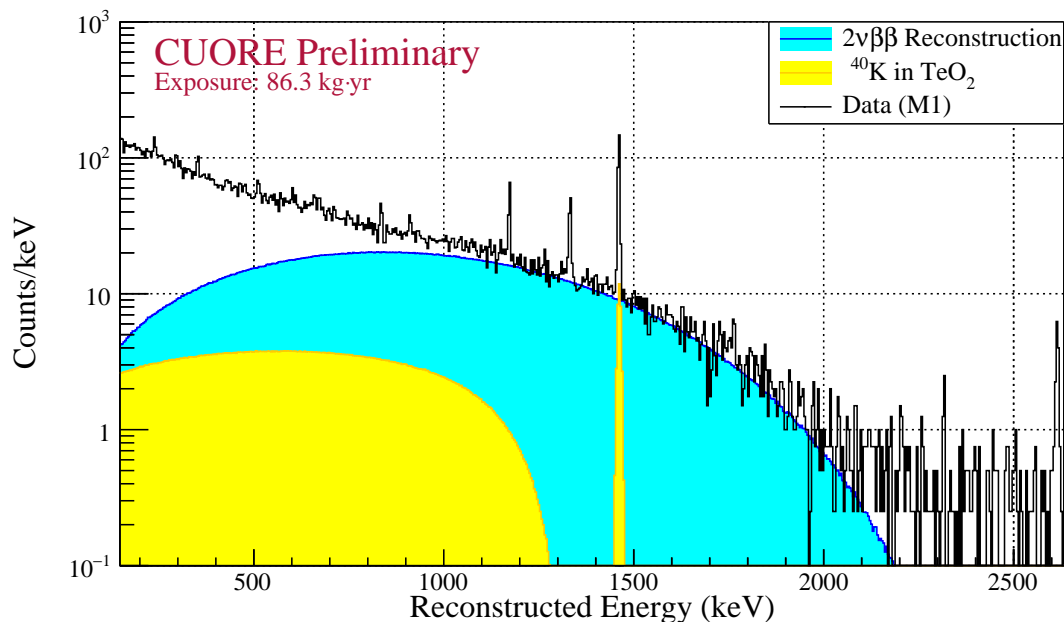


Figure 5. The observed MIL0 spectrum with the superposition of the $2\nu\beta\beta$ component (cyan) and ^{40}K (green). The $2\nu\beta\beta$ spectrum dominates the spectrum between 1 MeV and 2 MeV. Note: the binning has been changed for illustrative purpose, the actual fit has been performed with the binning used in Figure 4. Picture from [19].

5. Conclusions

CUORE, the first 1-ton scale array of bolometers searching for $0\nu\beta\beta$ began collecting data in summer of 2017. Using data collected in the first two datasets (24.0 kg · yr) of ^{130}Te of exposure, we set the strongest limit on the $0\nu\beta\beta$ decay half-life of ^{130}Te to date at $T_{1/2}^{0\nu} > 1.5 \times 10^{25}$ yr at 90% C.L. The same datasets were recently analyzed to reconstruct the background rate and we were able to perform a measurement of the $2\nu\beta\beta$ half-life: $T_{2\nu}^{1/2} = [7.9 \pm 0.1 \text{ (stat.)} \pm 0.2 \text{ (syst.)}] \times 10^{20}$ yr. This is the most precise measurement of the half-life of the $2\nu\beta\beta$ of ^{130}Te and one of the most precise measurements of any $2\nu\beta\beta$ rate.

Author Contributions: All the authors contributed equally to this work.

Funding: This work was supported by the Istituto Nazionale di Fisica Nucleare (INFN); the National Science Foundation under Grant Nos. NSF-PHY-0605119, NSF-PHY-0500337, NSF-PHY-0855314, NSF-PHY-0902171, NSF-PHY-0969852, NSF-PHY-1307204, NSF-PHY-1314881, NSF-PHY-1401832, and NSF-PHY-1404205; the Alfred P. Sloan Foundation; the University of Wisconsin Foundation; and Yale University. This material is also based upon work supported by the US Department of Energy (DOE) Office of Science under Contract Nos. DE-AC02-05CH11231, DE-AC52-07NA27344, and DE-SC0012654; and by the DOE Office of Science, Office of Nuclear Physics under Contract Nos. DE-FG02-08ER41551 and DE-FG03-00ER41138. This research used resources of the National Energy Research Scientific Computing Center (NERSC).

Acknowledgments: The CUORE Collaboration thanks the directors and staff of the Laboratori Nazionali del Gran Sasso and the technical staff of our laboratories.

Conflicts of Interest: The authors declare no conflict of interest.

References

1. Fukuda, S.; Fukuda, Y.; Ishitsuka, M.; Itow, Y.; Kajita, T.; Kameda, J.; Kaneyuki, K.; Kobayashi, K.; Koshio, Y.; Miura, M.; et al. Determination of solar neutrino oscillation parameters using 1496 days of Super-Kamiokande I data. *Phys. Lett. B* **2002**, *539*, 179–187. [[CrossRef](#)]
2. Ahmad, Q.R.; et al. [SNO Collaboration]. Measurement of the rate of $\nu_e + d \rightarrow p + p + e^-$ interactions produced by ^8B solar neutrinos at the Sudbury Neutrino Observatory. *Phys. Rev. Lett.* **2001**, *87*, 071301. [[CrossRef](#)]
3. Ahmad, Q.R.; et al. [SNO Collaboration]. Direct evidence for neutrino flavor transformation from neutral current interactions in the Sudbury Neutrino Observatory. *Phys. Rev. Lett.* **2002**, *89*, 011301. [[CrossRef](#)] [[PubMed](#)]
4. Eguchi, K.; et al. [KamLAND Collaboration]. First results from KamLAND: Evidence for reactor anti-neutrino disappearance. *Phys. Rev. Lett.* **2003**, *90*, 021802. [[CrossRef](#)] [[PubMed](#)]
5. Gando, A.; et al. [The KamLAND Collaboration]. Constraints on θ_{13} from A Three-Flavor Oscillation Analysis of Reactor Antineutrinos at KamLAND. *Phys. Rev. D* **2011**, *83*, 052002. [[CrossRef](#)]
6. Tanabashi, M.; et al. [Particle Data Group]. Review of Particle Physics. *Phys. Rev. D* **2018**, *98*, 030001. [[CrossRef](#)]
7. Alduino, C.; et al. [CUORE Collaboration]. First Results from CUORE: A Search for Lepton Number Violation via $0\nu\beta\beta$ Decay of ^{130}Te . *Phys. Rev. Lett.* **2018**, *120*, 132501. [[CrossRef](#)]
8. Agostini, M.; et al. [GERDA Collaboration]. Improved Limit on Neutrinoless Double- β Decay of ^{76}Ge from GERDA Phase II. *Phys. Rev. Lett.* **2018**, *120*, 132503. [[CrossRef](#)]
9. Gando, A.; et al. [KamLAND-Zen Collaboration]. Search for Majorana Neutrinos near the Inverted Mass Hierarchy Region with KamLAND-Zen. *Phys. Rev. Lett.* **2016**, *117*, 082503. [[CrossRef](#)]
10. Fischer, V. Search for Neutrinoless Double-Beta Decay with SNO+. In Proceedings of the 13th Conference on the Intersections of Particle and Nuclear Physics (CIPANP 2018), Palm Springs, CA, USA, 29 May–3 June 2018.
11. Albert, J.B.; et al. [EXO-200 Collaboration]. Search for Neutrinoless Double-Beta Decay with the Upgraded EXO-200 Detector. *arXiv* **2017**, arXiv:1707.08707.
12. Alfonso, K.; et al. [CUORE Collaboration]. Search for Neutrinoless Double-Beta Decay of ^{130}Te with CUORE-0. *Phys. Rev. Lett.* **2015**, *115*, 102502. [[CrossRef](#)] [[PubMed](#)]
13. Alduino, C.; et al. [CUORE Collaboration]. Analysis techniques for the evaluation of the neutrinoless double- β decay lifetime in ^{130}Te with the CUORE-0 detector. *Phys. Rev. C* **2016**, *93*, 045503. [[CrossRef](#)]
14. Andreotti, E.; et al. [CUORICINO Collaboration]. ^{130}Te Neutrinoless Double-Beta Decay with CUORICINO. *Astropart. Phys.* **2011**, *34*, 822–831. [[CrossRef](#)]
15. Arnaboldi, C.; et al. [CUORICINO Collaboration]. First results on neutrinoless double beta decay of Te-130 with the calorimetric CUORICINO experiment. *Phys. Lett. B* **2004**, *584*, 260–268. [[CrossRef](#)]
16. Arnaboldi, C.; et al. [CUORICINO Collaboration]. Results from a search for the 0 neutrino beta beta-decay of Te-130. *Phys. Rev. C* **2008**, *78*, 035502. [[CrossRef](#)]
17. Alduino, C.; et al. [CUORE Collaboration]. CUORE sensitivity to $0\nu\beta\beta$ decay. *Eur. Phys. J. C* **2017**, *77*, 532. [[CrossRef](#)]
18. Alduino, C.; et al. [CUORE Collaboration]. The projected background for the CUORE experiment. *Eur. Phys. J. C* **2017**, *77*, 543. [[CrossRef](#)]
19. Adams, D.Q.; et al. [CUORE Collaboration]. Update on the recent progress of the CUORE experiment. *arXiv* **2018**, arXiv:1808.10342.
20. Dell’Oro, S.; Alessandria, F.; Bucci, C.; Caminata, A.; Canonica, L.; Cappelli, L.; Cereseto, R.; Chott, N.; Copello, S.; Cremonesi, O.; et al. The CUORE cryostat: A 10 mK infrastructure for large bolometric arrays. *J. Phys. Conf. Ser.* **2017**, *888*, 012235. [[CrossRef](#)]
21. Alessandrello, A.; Brofferio, C.; Bucci, C.; Cremonesi, O.; Giulian, A.; Margesin, B.; Nucciotti, A.; Pavan, M.; Pessina, G.; Previtali, E.; et al. Methods for response stabilization in bolometers for rare decays. *Nucl. Instrum. Meth. A* **1998**, *412*, 454–464. [[CrossRef](#)]
22. Benato, G.; Biare, D.; Bucci, C.; Di Paolo, L.; Drobizhev, A.; Kadel, R.W.; Kolomensky, Yu.G.; Schreiner, J.; Singh, V.; Sipla, T.; et al. Radon mitigation during the installation of the CUORE $0\nu\beta\beta$ decay detector. *JINST* **2018**, *13*, P01010. [[CrossRef](#)]

23. Agostinelli, S.; et al. [Geant4 Collaboration]. Geant4—A simulation toolkit. *Nucl. Instr. Meth. A* **2003**, *506*, 250–303.
24. Alduino, C.; et al. [CUORE Collaboration]. Measurement of the two-neutrino double-beta decay half-life of ^{130}Te with the CUORE-0 experiment. *Eur. Phys. J. C* **2017**, *77*, 13. [[CrossRef](#)]
25. Plummer, P. JAGS User's Manual. Available online: <http://mcmc-jags.sourceforge.net> (accessed on 31 December 2018).
26. Gelman, A.; Carlin, J.; Stern, H.; Dunson, D.; Vehtari, A.; Rubin, D. *Bayesian Data Analysis*; Texts in Statistical Science: New York, NY, USA, 2014.
27. Arnold, R.; et al. [NEMO-3 Collaboration]. Measurement of the Double Beta Decay Half-life of ^{130}Te with the NEMO-3 Detector. *Phys. Rev. Lett.* **2011**, *107*, 062504. [[CrossRef](#)] [[PubMed](#)]



© 2019 by the authors. Licensee MDPI, Basel, Switzerland. This article is an open access article distributed under the terms and conditions of the Creative Commons Attribution (CC BY) license (<http://creativecommons.org/licenses/by/4.0/>).